Open access • Journal Article • DOI:10.1007/S10853-013-7526-Z

Low temperature TLP bonding of Al2O3–ceramics using eutectic Au–(Ge, Si) alloys

Nico Weyrich, Christian Leinenbach

Institutions: Swiss Federal Laboratories for Materials Science and Technology

Published on: 21 Jun 2013 - Journal of Materials Science (Springer US)

Topics: Eutectic bonding, Soldering, Eutectic system, Wetting and Differential scanning calorimetry

Low temperature TLP bonding of Al2O3-ceramics using eutectic Au-(Ge, Si) alloys

Author(s):
Weyrich, N.; Leinenbach, C.

Publication date:
2013

Permanent link:
https://doi.org/10.3929/ethz-b-000070713

Originally published in:
Journal of Materials Science 48(20), https://doi.org/10.1007/s10853-013-7526-z

J Mater Sci (2013) 48:7115–7124
DOI 10.1007/s10853-013-7526-z

Low temperature TLP bonding of Al_2O_3–ceramics using eutectic Au–(Ge, Si) alloys

Nico Weyrich · Christian Leinenbach

Received: 20 March 2013 / Accepted: 11 June 2013 / Published online: 21 June 2013

Abstract In this study, Al_2O_3–ceramics were joined via TLP bonding using interlayers of eutectic Au–12Ge (wt%) and Au–3Si (wt%) solder alloys, respectively, with a melting temperature of 361 and 363 °C and Ni wetting layers. The Ni layers were part of a metallic multilayer coating (Ti/W/Ni) applied on the ceramic surface to ensure wetting and adhesion during the joining process. For comparison, a soldering process was performed as well by changing the multilayer structure to Ti/W/Au. With respect to the different joining processes the influence of the variation in wetting layers on the interface reactions, mechanical properties and re-melting temperature was analyzed by scanning electron microscopy, shear testing, and differential scanning calorimetry. It is shown that sound joint can be produced at a joining temperature of 400 °C, achieving reasonable shear strength and re-melting temperatures more than 550 °C above the initial melting temperature of the filler metal.

Introduction

Due to their excellent properties such as high hardness, high compression strength, low density, high melting temperatures and low thermal expansion, as well as good resistance to many chemicals and biocompatibility, ceramics are favored in many advanced functional devices in high power electronics, biomedical engineering, and aerospace technology. However, because of functional or geometrical reasons it is for many applications not possible to form the structural component monolithically. Therefore, reliable and well assessed joining processes are required to produce sound ceramic–ceramic joints as well as multimaterial assemblies.

For joining of ceramics several techniques are available including solid-state diffusion bonding [1], friction joining [2], laser welding [3], ultrasonic joining [4], and brazing [5]. Most of these joining processes involve high temperatures which may be detrimental for components with heat-sensitive properties. To overcome this problem, transient-liquid-phase (TLP) bonding has been developed which combines low joining temperatures with high re-melting temperatures of the joints at the same time. In TLP bonding metallic interlayers are used that melt at a sufficiently low joining temperature. Via diffusion of the interlayer elements into the base material and/or vice-versa new phases with a higher melting point form, leading to isothermal solidification [6, 7]. The re-melting temperature of the joints exceeds the initial bonding temperature.

For TLP bonding of ceramics diverse interlayer systems have been proposed. Most of the multilayer structures investigated so far rely on so called partial transient liquid phase bonding (PTLP). In PTLP bonding thin films of a low melting point metal or alloy are deposited onto a much thicker layer of a refractory metal. At the joining temperature, the low melting material melts and wets the ceramic surface while concomitantly diffusing into the solid refractory core [6, 8]. Following this approach still requires high process temperatures that commonly exceed 1000 °C as well as long process times mostly in the range of several hours.

N. Weyrich (✉) · C. Leinenbach
Laboratory for Joining Technologies and Corrosion, Empa—Swiss Federal Laboratories for Materials Science and Technology, Überlandstrasse 129, 8600 Dübendorf, Switzerland
e-mail: nico.weyrich@empa.ch

C. Leinenbach
e-mail: christian.leinenbach@empa.ch

Different interlayer structures containing Cu as a low melting material have been analyzed such as Cu–Pt–Cu [8], Cu–Ni–Cu [9], and Cu–Nb–Cu [10, 11]. Besides the fact that high mean flexure strength values between 159 and 181 MPa could be achieved, the big disadvantage of these systems is the required joining temperature of 1150 °C for a dwell time of up to 6 h. Even higher temperatures of 1400°C are needed when Ni–Nb–Ni interlayer are used [12, 13]. Hong et al. investigated this system comparing various dwell times between 5 min and 6 h. Since the joints did not show big differences it was concluded that the liquid completely disappears after 5 min at joining temperature and they introduced the expression of (ultra-)rapid TLP bonding [12, 13].

In order to go to lower joining temperatures Chang et al. followed another approach in TLP bonding of alumina [14, 15]. Instead of using metallic interlayer, they implemented a glassy low melting boron oxide layer. At joining temperature of 800 °C and a comparably long dwell time of 15 h the boron oxide layer melted and reacted with alumina to form a stable high temperature compound. Even lower joining temperatures can be reached employing In as a melting point depressant [16, 17]. Lin et al. [17] used In as melting point suppressant when joining Al_2O_3 by means of a Ag thick film. The advantages of this technique are very low joining temperatures (180–250 °C) and fast processing times (1–6 min), while the main disadvantage is the very low shear strength between 0.75 and 1.4 MPa.

In this study, Au–12Ge was used, which has already proven to be an appropriate filler metal to join ceramics. Leinenbach et al. achieved mean shear strength values of up to 55 MPa when joining Al_2O_3 substrates using Au–12Ge in combination with a Cr–Ni/Ti–W/Au coating of the ceramics. The joining temperature was as low as 400 °C, requiring a short dwell time of 10 min [18]. Au–12Ge has also been used to join pure Ni, where it first showed a TLP bonding like behavior [19]. During the joining process, a Ni–Ge reaction layer formed at the solder–substrate interfaces and almost pure Au was detected around the center line of the joint when the Au–12Ge layer was sufficiently thin. This indicated that isothermal solidification took place due to the fact that phases with a higher melting temperature developed.

In this study, Au–12Ge and Au–3Si solder alloys were used as interlayer in combination with different multilayer coatings of the ceramics. Au–12Ge and Au–3Si both are interesting for joining because besides their low melting temperatures of 361 and 363 °C, respectively, they offer a lot of other beneficial features such as good corrosion resistance, good thermal and electrical conductivity as well as good mechanical properties. The resulting joints were analyzed with respect to the underlying joining process and its impact on microstructure and joint properties.

Materials and methods

For this study, sintered polycrystalline high-purity Al_2O_3 plates (Kyocera A-493; Kyocera, Esslingen, Germany) with a thickness of 0.64 mm were used as substrates. According to the manufacturer, the ceramics exhibit a tensile strength of 320 MPa, a grain size smaller than 1.5 µm and a surface roughness of Ra 5 µm. Two multilayer coatings consisting of 30 nm Ti, 100 nm W, 2 µm Ni and 30 nm Ti, 100 nm W, 1 µm Au were deposited on the ceramic surface by sputtering (Thinfilms Inc., Hillborough, New Jersey) (Fig. 1). In this systems Ni and Au, respectively, were used as top layers to provide sufficient wetting by the Au-based solder alloys. In addition to this a Ti layer was introduced to promote adhesion as it can react with the ceramic during joining to form different oxides [20] or Ti[Al, O] solid solution and Ti_3Al[O] [21, 22]. In order to prevent Ti from diffusing to the metallization–solder interface and from reacting with the solder, W was used as a diffusion barrier.

For joining the coated ceramics were cut via laser cutting into pieces of 20 × 10 mm and 4 × 4 mm. The Au–12Ge (wt%) and Au–3Si (wt%) solder foils (thickness 25 µm) were provided by Materion (Buffalo, New York) and cut by laser cutting into pieces 5 × 5 mm in size. Figure 2 shows the corresponding binary phase diagrams of (a) Au–Ge and (b) Au–Si [23].

All the materials were carefully cleaned in soap water, distillated water and high-purity acetone prior to joining. For joining a specially designed jig was used to keep the components in position and prevent floating or rotating. Small pieces of coated ceramics (4 × 4 mm) were placed on larger plates (20 × 10 mm) with a solder foil (5 × 5 mm) in between. The bonding process was performed in a vacuum furnace (Cambridge Vacuum Engineering, Model 1218H, Cambridge, UK) at 400 °C and a pressure of 10^{-4} Pa using dwell times of 10 and 30 min. After joining the remelting temperature of the bonds was measured via differential scanning calorimetry (DSC

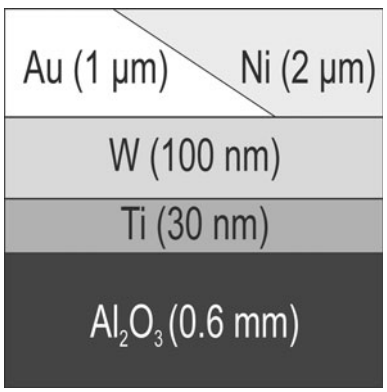

Fig. 1 Multilayer structure of Ti/W/Au or Ti/W/Ni on Al_2O_3

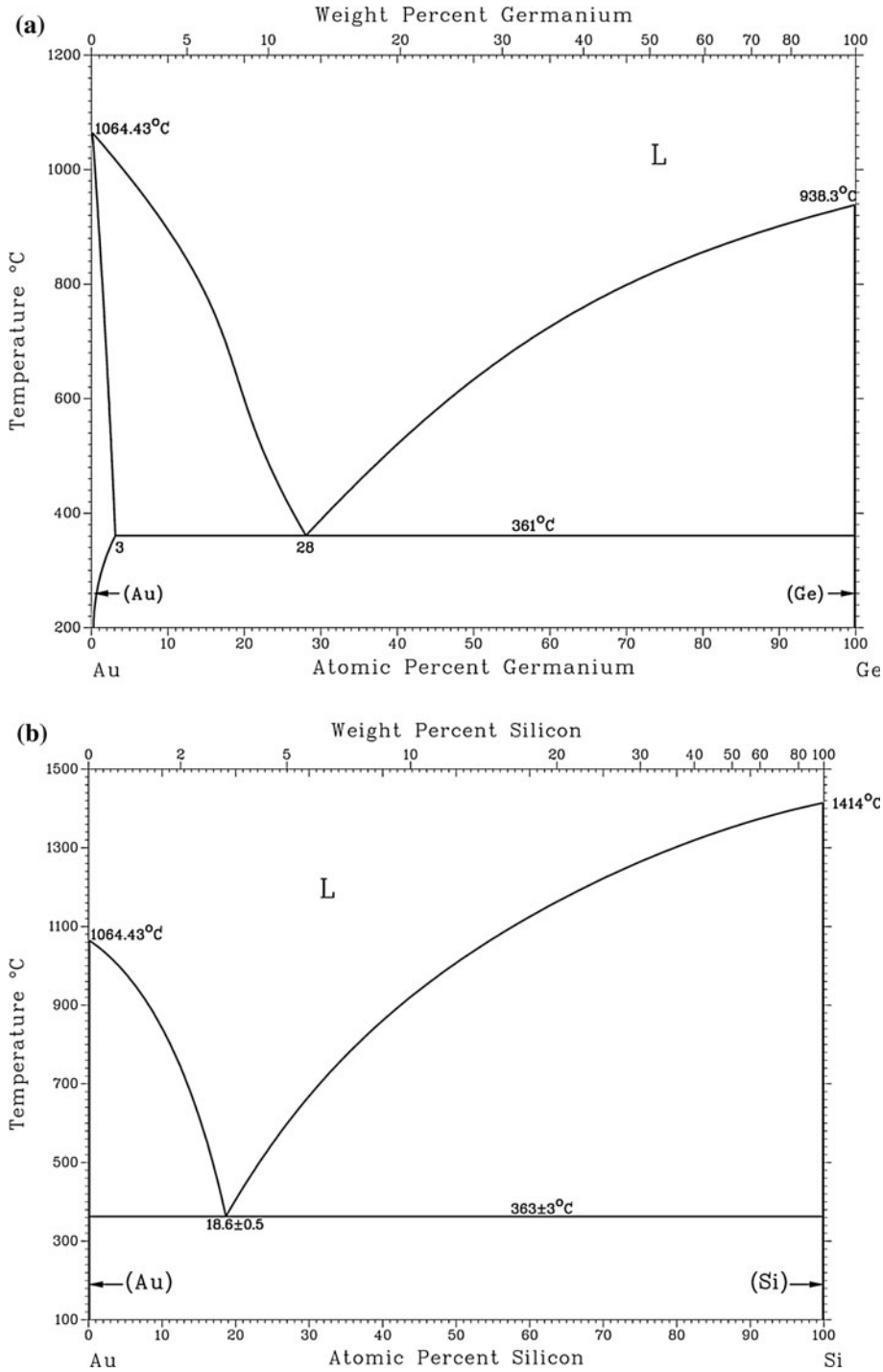

Fig. 2 Binary phase diagrams of **a** Au–Ge and **b** Au–Si

Netzsch DSX 404 F3 Pegasus, Erich NETZSCH, Selb, Germany). Therefore, specimens of 3 × 3 mm were cut out of the joined samples using a diamond blade. These smaller samples were heated to 1100 °C at a heating rate of 10 °C min^{-1} and afterward cooled down to room temperature in an Al_2O_3 crucible under high-purity Ar-atmosphere while the resulting heat flow was recorded. The melting temperature was defined at the point where the DSC signal showed the first endothermal deviation from the base line.

For the investigation of the microstructure bonded samples were mounted in epoxy resin, ground and polished for Scanning Electron Microscope (SEM; ESEM XL 30, FEI, Eindhoven, Netherlands) observation. The SEM was equipped with an Energy Dispersive X-ray (EDS) detector to do semi-quantitative chemical analysis.

In addition to that the mechanical properties of the joints were evaluated by means of shear tests and micro-hardness measurements. A STM-20A shear test device (Walter + Bai AG, Loehningen, Switzerland) was employed. Samples were adjusted in the machine in a way that the load was introduced approximately 50 μm above the solder–ceramic interface parallel to the substrate (for shear test setup, see [19]). Tests were carried out under displacement control with a shear rate of 0.1 mm s^{-1}. Shear strength was calculated at the maximum load ($\tau = F_{max}/A$; $A = 16$ mm^2). Hardness measurement were conducted on a Fischerscope HM2000 (Helmut Fischer GmbH, Sindelfingen, Germany) micro-hardness tester using a standard Vickers type diamond tip indenter. The indentation load was set to 10 mN for a duration of 20 s.

Results

Microstructure and re-melting temperature

In order to compare the microstructure of the solder before and after joining, the solder foils were investigated in the as delivered condition. Figure 3 shows the microstructures of the (a) Au–12Ge and (b) Au–3Si solder foils prior to soldering. For both alloys, the matrix consists of Au and appears almost white in the backscattered electron (BSE) image. Coarse Ge grains of different sizes from 1 to 3.5 μm in diameter were present in the Au–12Ge solder foil with no homogeneous distribution (a). In contrast to that, the Si grains were dispersed homogeneously within the Au–3Si alloy. The Si grains were much smaller reaching a maximum size of 1 μm (b).

Figure 4 shows the microstructures obtained when joining Al_2O_3 ceramics coated with Ti, W, and Au and using (a) Au–12Ge and (b) Au–3Si eutectic solder as interlayer. In these micrographs, the Ti and W layers are not distinguishable due to the limited resolution of the SEM in the BSE mode. However, in the areas indicated in white dotted lines these elements have been detected by EDS which indicates that no pronounced diffusion into the solder alloy and no reaction with the solder have taken place. For the Au–12Ge interlayer the soldering gap has an average size of 9.9 μm and consists of Au with Ge grains up to a dimension of 3.4 μm (a). During the joining process separation of the elements took place, but in some areas the eutectic structure is still present. A eutectic structure can also be seen in Fig. 4b when Au–3Si was employed as a filler metal. Compared to the solder in the as delivered condition (see Fig. 3b) a coarsening of the Si grains took place during the joining process. After joining, the Si grains showed an average width of 0.5 μm and length of 3.1 μm. The mean width of the soldering gap was measured to 11.5 μm.

Table 1 shows a summary of the average size of the soldering gaps and compound sizes for the following different material combinations and process parameters. In these joints Al_2O_3–ceramics coated with Ti, W and Ni were used, while the solder was varied. Figure 5 shows the micrograph of a joint using an Au–12Ge interlayer. During joining the eutectic structure of the solder alloy disappeared completely while the elements separated to form Ni–Ge intermetallics (IMCs) and a pure Au layer, respectively. The soldering gap had an average width of 13.1 μm and was enclosed to both sides by a Ni–Ti–W layer. As can be seen in Fig. 5, this layer was followed by a 0.9-μm thick Ni_5Ge_3 IMC layer upon which the NiGe phase formed. The average NiGe layer thickness was 2.2 μm while some bigger grains (up to 4 μm) reached into the center area of the joint. Around the centerline a 7.2 μm wide area consisting of pure Au was observed. For the two reaction phases the micro-hardness values were determined to be

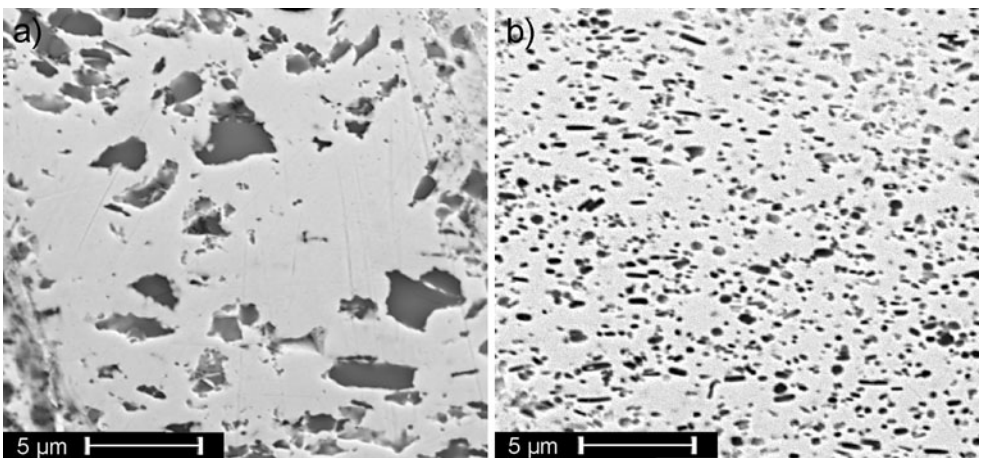

Fig. 3 Microstructure of the **a** Au–12Ge and **b** Au–3Si solder foils

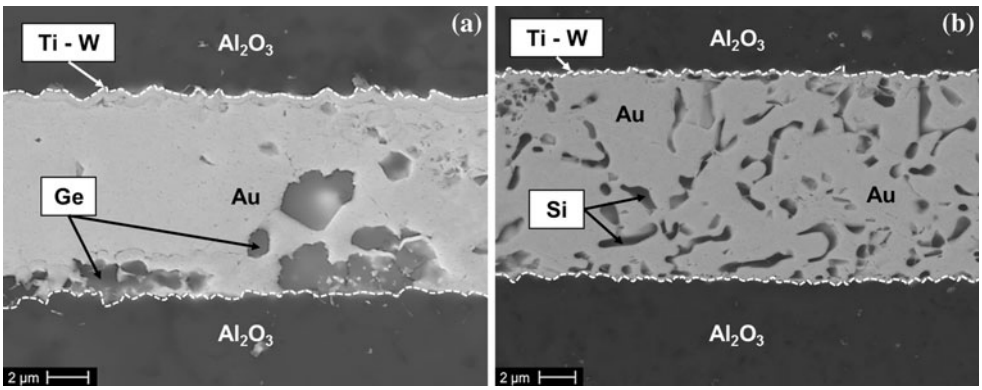

Fig. 4 Microstructure of Al_2O_3/Ti/W/Au joined with **a** Au–12Ge and **b** Au–3Si at $T = 400$ °C, $t = 10$ min

Table 1 Average soldering gap and compound size (µm) for different material combinations and process parameters

	Soldering gap	Central Au layer	Ni_5Ge_3	NiGe	Ni_3Si	NiSi	Ni_3Si_2	Si grains	Ratio IMC/Au (%)
Al_2O_3/Ti/W/Ni Au–12Ge (400 °C/10 min)	13.1	7.2	0.9	2.2	–	–	–	–	86
Al_2O_3/Ti/W/Ni Au–3Si (400 °C/10 min)	8.9	6.3	–	–	0.6	0.7	–	0.3–2	41
Al_2O_3/Ti/W/Ni Au–3Si (400 °C/30 min)	8.8	5.5	–	–	0.8	–	0.9	–	62

759 HV for Ni_5Ge_3 and 1028 HV for NiGe. The Au phase was much softer and reached a hardness of 162 HV.

For Al_2O_3/Ti/W/Ni bonded with Au–3Si two different dwell times (Fig. 6a 10 min; Fig. 6b 30 min) were tested resulting in slightly different microstructures, whereas the width of the soldering gap was almost the same (8.8 and 8.9 µm). In both cases, Ti and W were detected on the Al_2O_3 surfaces with no pronounced diffusion into the solder alloy. For a dwell time of 10 min a Ni–Ti–W layer is followed by a 0.6-µm thick Ni_3Si and a 0.7-µm thick NiSi reaction layer. The middle part of the soldering gap is 6.3 µm wide and comprises almost pure Au with several separated grains. These 0.3–2 µm big grains are believed to consist of Si suggesting that in some areas the eutectic structure is still present. A dwell time of 30 min resulted in two reaction layers composed of Ni_3Si and Ni_3Si_2 with a thickness of 0.8 and 0.9 µm, respectively. 5.5 µm of pure Au were found around the centerline of the joint whereas the Si grains were no longer present. Overall the ratio of IMC to Au thickness was 21 points higher after a dwell time of 30 min compared to 10 min and reached a value of 62 %. Micro-hardness measurements revealed a value of 326 HV for the Ni_3Si phase.

To determine the re-melting temperature of the joints DSC measurements have been conducted. Figure 7 shows the obtained results for joints produced with Au–12Ge and

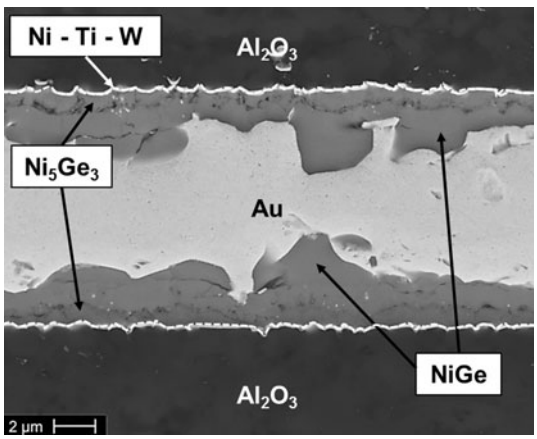

Fig. 5 Microstructure of Al_2O_3/Ti/W/Ni joined with Au–12Ge at $T = 400$ °C, $t = 10$ min

Au–3Si eutectic solders and a Ti/W/Au coating on the Al_2O_3 substrates. For both solder alloys the measured re-melting temperature of the joints is close to the initial melting temperature of the eutectic alloy (Au–12Ge: 361 °C/Au–3Si: 363 °C). This confirms the results obtained in EDS analyses which suggested that the eutectic structure is still present in some areas of the soldering zone. The same assumption holds for the Al_2O_3/Ti/W/Ni joints using Au–3Si interlayer and a dwell time of 10 min. In this case, the re-melting temperature of 365 °C can also be referred to

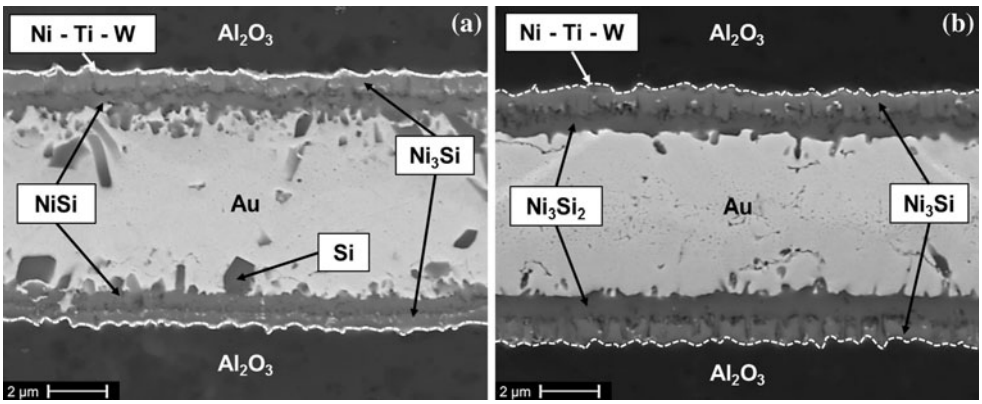

Fig. 6 Microstructure of Al_2O_3/Ti/W/Ni joined with Au–3Si at **a** $T = 400$ °C, $t = 10$ min and **b** $T = 400$ °C, $t = 30$ min

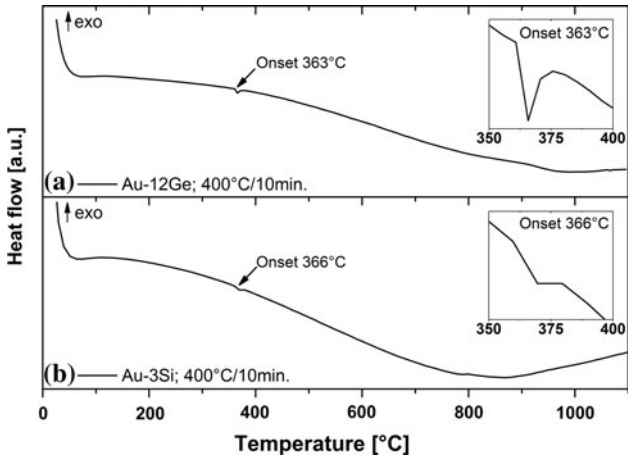

Fig. 7 DSC curves for the determination of the re-melting temperature of Al_2O_3/Ti/W/Au joined with **a** Au–12Ge and **b** Au–3Si at $T = 400$ °C, $t = 10$ min

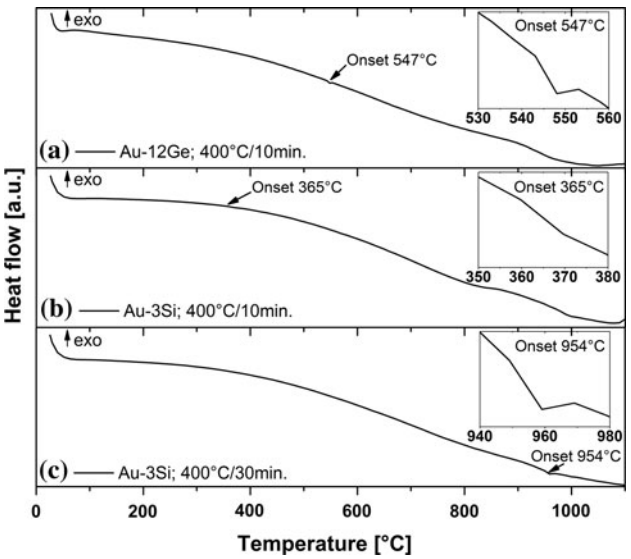

Fig. 8 DSC curves for the determination of the re-melting temperature of Al_2O_3/Ti/W/Ni joined with **a** Au–12Ge, **b** Au–3Si at $T = 400$ °C, $t = 10$ min and **c** Au–3Si at $T = 400$ °C, $t = 30$ min

residuals of the eutectic structure of the solder alloy (Fig. 8b). As can be seen in Fig. 8a and c neither for Au–12Ge (400 °C/10 min), nor for Au–3Si (400 °C/30 min) melting was detected at the initial melting temperature of the solder alloys. For the joints produced using Au–12Ge an endothermal peak caused by melting of one of the compounds was found at 547 °C. When Au–3Si was applied as a filler metal and the dwell time was set to 30 min the re-melting temperature of the joints was 954 °C, which is 554 °C above the joining temperature.

Shear strength and fracture behavior

For the determination of the mechanical properties shear tests were conducted. Figures 9 and 11 show the shear test results displayed in a box plot diagram. The dots besides the box represent the single test values, while the box indicates the 25th and 75th percentile, that is, the shear stress at which 25 and 75 % of the tested samples failed. Mean values are presented by dots within the boxes. Using an Au-wetting layer and Au–12Ge solder alloy (Fig. 9) lead to shear strength values between 34 and 64 MPa. The mean value was calculated to 51 MPa, while the standard deviation was 12 MPa. An analysis of the fracture surfaces revealed almost pure Au on both of the fractured parts (Fig. 10a). Underneath the Au-rich structures Ti and W were detected on the ceramic surface. This indicates a cohesive fracture behavior with a crack propagating through the middle of the soldering gap. When the interlayer was changed to Au–3Si mean shear strength slightly decreased to 47 MPa, whereas the scattering also decreased approaching a standard deviation of 8 MPa. For the majority of the samples cohesive fracture took place in the Au-rich area in the middle of the soldering gap. Besides spherical drop-like particles of pure Au, structures consisting of Au and traces of Si were detected on both of the fracture surfaces (Fig. 10b).

When the Ti/W/Ni coating system was applied the mean shear strength values were marginally higher, all in the

range of 55 MPa (Fig. 11). For an Au–12Ge interlayer the strength of the joints mainly ranged between 35 and 65 MPa with an outlier at 93 MPa. When all single values were taken into account a standard deviation of 16 MPa was calculated. In these joints the fracture path was determined to run along the interface between the Ni–Ti–W layer and the Ni_5Ge_3 phase on one of the substrates which seems to be the weak point. On one of the fractured parts an almost continuous layer of Ni_5Ge_3 was found (Fig. 12a), while on the other part the elements Ni, Ti, and W were detected. Choosing Au–3Si as an interlayer a variation in the dwell time had no significant influence on the shear strength and fracture behavior. The average shear strength in both cases was 55 MPa with a standard deviation of 19 MPa (400 °C/10 min) and 16 MPa (400 °C/30 min), respectively. The fracture behavior was also similar for both dwell times. Figure 12b shows that the solder and the Ni-rich reaction layers stayed on one of the substrates after fracture with Ni_3Si on top. Thus, it was concluded that the fracture path followed the interface between Ni_3Si and the Ni–Ti–W layer.

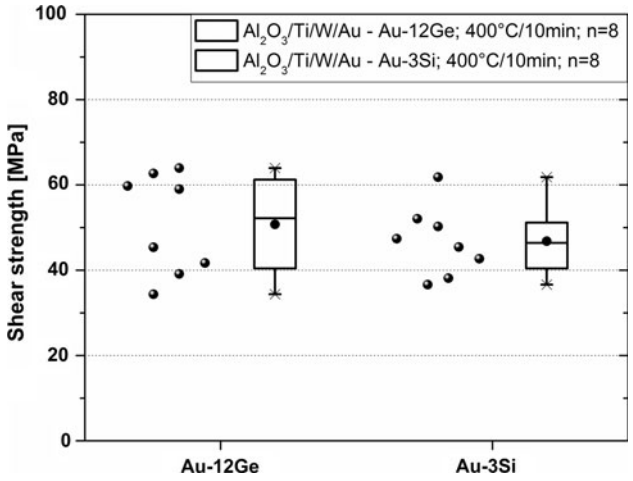

Fig. 9 Shear strength of Al_2O_3/Ti/W/Au joined with Au–12Ge and Au–3Si

Discussion

Microstructure and joining process

Microstructural analysis and the associated DSC measurement of the re-melting temperature of the joints showed the characteristics of a soldering process when a Ti/W/Au coating was applied. Sound joints are reached by the melting and flowing of the filler metal. Since some amount of the solder alloys flew out of the soldering gap its width was generally less than the initial thickness of the solder foils. To some extent a separation of the solder elements associated with a coarsening of the grains took place during joining, but the eutectic structure was still present in some areas. Therefore, the re-melting temperature of the joints did not exceed the initial melting temperatures of the solder alloys. For a Ti/W/Ni coating in combination with Au–3Si and a dwell time of 10 min a significant reaction of Ni and Si was found. Two reaction layers (NiSi and Ni_3Si) formed but obviously the dwell time was too short for an entire reaction of Ni and Si. Thus, some grains of pure Si remained and the eutectic structure did not vanish completely. As a consequence the re-melting temperature of the joints was similar to the melting point of the eutectic Au–3Si alloy.

A TLP bonding process was performed for a Ni wetting layer in combination with Au–12Ge and Au–3Si (400 °C/30 min). Ge and Si strongly react with Ni to form new phases (Ni_5Ge_3, NiGe and Ni_3Si, Ni_3Si_2, respectively) and therefore Ge/Si are diffusing out of the filler metal and to the Ni layer. As a consequence, the eutectic structure of the

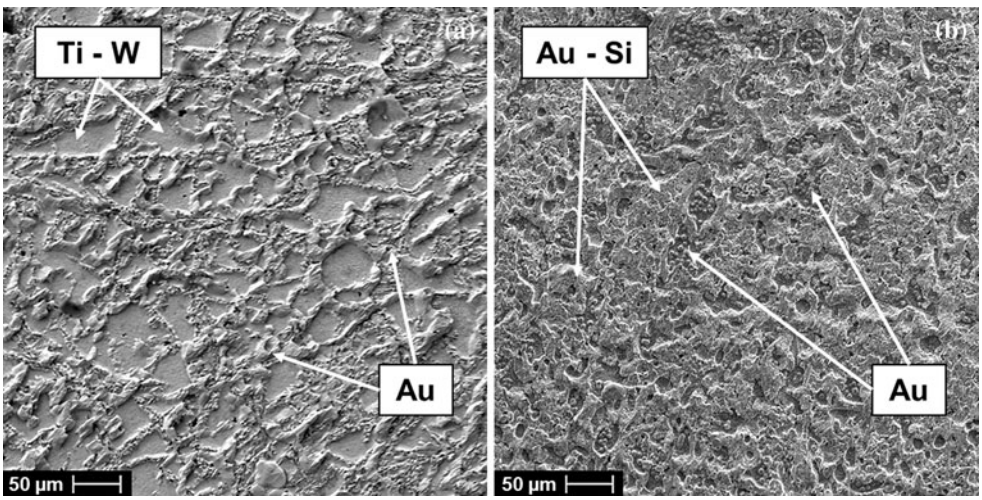

Fig. 10 Fracture surfaces of Al_2O_3 joined with **a** Au–12Ge and **b** Au–3Si

solder alloys disappears. Due to the fact that the newly forming phases have a higher melting temperature than the joining temperature of 400 °C isothermal solidification takes place. Isothermal solidification requires an entire reaction of Ge/Si with Ni which is not only dependent on the process parameters but also on the thickness of solder foil and wetting layers. Therefore, the maximum thickness of the Au–12Ge and Au–3Si foils in combination with 2-µm thick Ni layer on both sides was calculated. Given the mean thickness of the IMC layers in the observed joints the number of Ge and Si atoms, respectively, was determined. Based on the number of Ge/Si atoms that were incorporated in the IMC layers, the maximum thickness of the Au–12Ge/Au–3Si foil was calculated. The resulting thickness was 13.95 µm for Au–12Ge and 12.26 µm for Au–3Si, which corresponds to a thickness ratio of 3.49 for Au–12Ge to Ni and 3.07 for Au–3Si to Ni. These are theoretical values valid for closed systems where no solder material is able to flow out of the soldering gap. In the presented systems 45 % (Au–12Ge) and 51 % (Au–3Si) of the solder alloy flew out of the soldering gap and as a consequence an initial thickness ratio of 4–25 µm from wetting layer to solder foil lead under the given conditions to complete isothermal solidification and high re-melting temperatures.

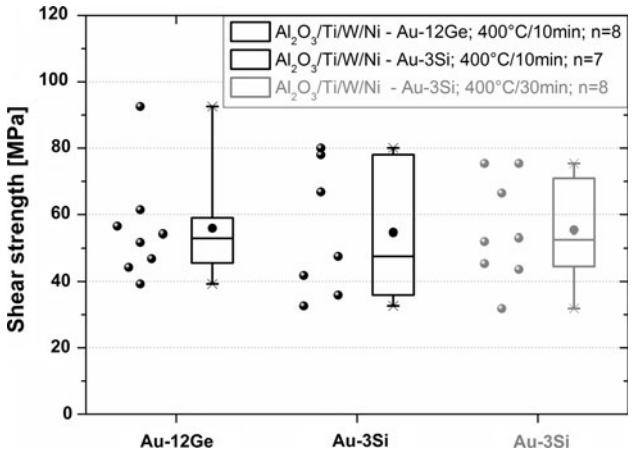

Fig. 11 Shear strength of Al_2O_3/Ti/W/Ni joined with Au–12Ge and Au–3Si

When Au–12Ge was used as a filler metal the re-melting temperature was identified at 547 °C. This value corresponds to the temperature of the $NiGe + Ni_5Ge_3 + Au \leftrightarrow L + Au + Ni_5Ge_3$ reaction which was found in [24]. It is also referred to as the invariant temperature of the reaction $L + Ni_5Ge_3 \leftrightarrow NiGe + fcc$ [24]. For an Au–3Si interlayer the re-melting temperature was 954 °C. In the binary phase diagrams no associated melting point was found and since no information about the Au–Ni–Si ternary system is available the melting compound remains currently unclear.

Based on these results, the joining process has been illustrated in Fig. 13 for the TLP bonding via Au–12Ge or Au–3Si eutectic solder interlayer in combination with a Ni metallization layer. Figure 13a shows the basic assembly of the components to be joined. The two coated ceramics with a Ni top-layer are sandwiched with a eutectic solder foil in between. When the assembly is heated to joining temperature the solder interlayer melts. Thus, Ge and Si, respectively, diffuse to the solder–coating interface and into the Ni layer causing a separation of the elements (Fig. 13b). As a consequence reactions take place and new phases with a higher melting temperature are formed leading to isothermal solidification (Fig. 13c). The solidification of the joint is due to two different events and occurs in two different directions. While the IMC phases grow in direction of the center line of the joint, pure Au accumulates in the center and grows in the opposite direction. Due to this two-directional solidification the

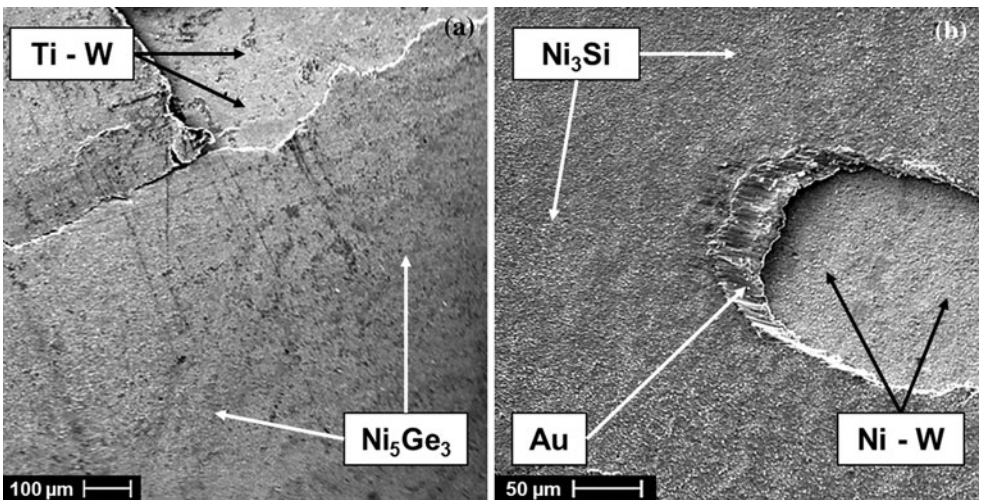

Fig. 12 Fracture surface of Al_2O_3/Ti/W/Ni joined with **a** Au–12Ge and **b** Au–3Si

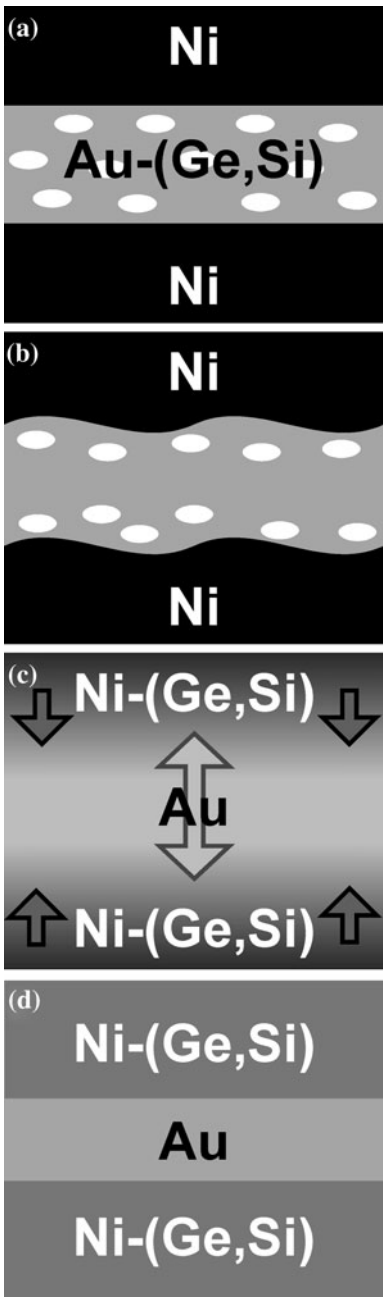

Fig. 13 Joining process for TLP bonding with Au–(Ge, Si) in contact with Ni wetting layers: **a** assembly before joining, **b** above T_m of Au–(Ge, Si), **c** reaction and isothermal solidification, **d** solidified joint

solid state is reached very fast, which gives an explanation for the short process times of 10 and 30 min. The final joint consists of reaction layers of Ni–Ge or Ni–Si, respectively, and a pure Au layer around the centerline (Fig. 13d). Re-melting temperatures therefore are much higher than the initial joining temperature.

For the Au–Ge–Ni system, these reactions have been exemplary studied more in detail using the available ternary phase diagram [24]. Figure 14 shows an isothermal

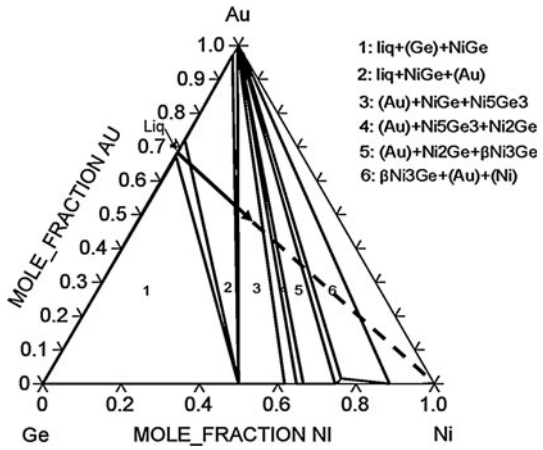

Fig. 14 Reaction path in an isothermal section of the Au–Ge–Ni phase diagram at 400 °C

section of the Au–Ge–Ni phase diagram at 400 °C. The arrow shows the reaction path of the joining process starting in the eutectic Au–12Ge liquidus region leading in the direction of pure Ni. At first the formation of NiGe starts and phase field number 2 is reached where liquid Au–12Ge, NiGe and Au exist simultaneously. At a certain point the formation of Ni_5Ge_3 is thermodynamically more favorable approaching the composition of phase field number 3. In this field Au, NiGe and Ni_5Ge_3 coexist and isothermal solidification is completed.

Strength and fracture behavior

Overall reasonable shear strength values could be achieved with both filler metals and metallization systems. When an Au-wetting layer was applied fracture strength and fracture behavior did not vary significantly for the two filler metals. In both cases, the average shear strength was around 50 MPa. The fracture surface showed the characteristics of a cohesive fracture in the middle of the soldering gap. Apparently, the shear strength of the Au matrix containing brittle Ge or Si grains was below the shear strength at the solder–ceramic interface and therefore the crack propagated in the Au-rich area.

For the coating system with a Ni wetting layer shear strength were slightly higher compared to the Au-wetting layer and the fracture behavior changed from cohesive to adhesive fracture. The crack no longer proceeded in the Au-rich part of the joint, but along the reaction layer–coating interface. Even though the ratio from IMCs to Au-layer thickness was very high (86 %) in joints with an Au–12Ge interlayer, the IMCs were not detrimental for the joint strength. The weak point of these joints was the connection between the Ni_5Ge_3 layer and a layer composed of a mixture of Ni, Ti, and W. Similar results were obtained

using Au–3Si filler alloys, when the joints failed at the interface between Ni_3Si and a Ni–Ti–W layer.

Conclusion

In conclusion, Au–12Ge and Au–3Si eutectic solder alloys have proven to be possible interlayer materials to join Al_2O_3 ceramics at low temperatures ($T = 400$ °C). The combination of these Au-based alloys with a multilayer metallization consisting of Ti/W/Au or Ti/W/Ni, respectively, leads to sound joints with reasonable shear strength. It has been shown that a soldering process as well as a TLP bonding process can be realized just by changing the wetting layer material, which has a big influence on the microstructure and re-melting temperature. Re-melting temperatures of the joints produced via TLP bonding were more than 550 °C above the initial joining temperature which makes them suitable for high temperature applications. Compared to other TLP bonding techniques known in literature the use of Au–12Ge and Au–3Si possesses the big advantage of low joining temperature and fast processing times which minimizes the thermal impact on the components. As a consequence this process is suitable for joining of components with heat-sensitive properties, as well as for bonding of dissimilar materials with a mismatch in thermal expansion coefficients.

References

1. Akselsen OM (1992) J Mater Sci 27:569. doi:10.1007/BF02403862
2. Rashid H, Hunt KH, Evans JRG (1991) J Eur Ceram Soc 8:329
3. Lippmann W, Knorr J, Wolf R, Rasper R, Exner H, Reinecke AM, Nieher M, Schreiber R (2004) Nuc Eng Des 231:151
4. Iijima M, Watanabe Y (2003) Jap J Appl Phys 42:2986
5. Yong Z, Feng D, Zhi-Yong H, Xi-Chun C (2006) J Iron Steel Res 13:1
6. Cook GO, Sorensen CD (2011) J Mater Sci 46:5305. doi:10.1007/s10853-011-5561-1
7. Gale WF, Butts DA (2004) Sci Technol Weld Join 9:283
8. Shalz ML, Dalgleish BJ, Tomsia AP, Glaeser AM (1993) J Mater Sci 28:1673. doi:10.1007/s10853-011-5324-z
9. Shalz ML, Dalgleish BJ, Tomsia AP, Glaeser AM (1994) J Mater Sci 29:3200. doi:10.1007/BF00356663
10. Shalz ML, Dalgleish BJ, Tomsia AP, Cannon RM, Glaeser AM (1994) J Mater Sci 29:3678. doi:10.1007/BF00357335
11. Marks RA, Sugar JD, Glaeser AM (2001) J Mater Sci 36:5609. doi:10.1023/A:1012565600601
12. Hong SM, Bartlow CC, Reynolds TB, McKeown JT, Glaeser AM (2008) Adv Mater 20:4799
13. Hong SM, Reynolds TB, Bartlow CC, Glaeser AM (2010) Int J Mater Res 101:133
14. Chang LS, Huang CF (2004) Ceram Int 30:2121
15. Lo PL, Chang LS, Lu YF (2009) Ceram Int 35:3091
16. Hong SM, Glaeser AM (2006) In: Proceedings of International Brazing and Soldering Conference 181–188
17. Lin JC, Huang LW, Jang GY, Lee SL (2002) Thin Solid Films 410:212
18. Leinenbach C, Weyrich N, Elsener HR, Gamez G (2012) Int J Appl Ceram Technol 9:751
19. Leinenbach C, Valenza F, Giuranno D, Elsener HR, Jin S, Novakovic R (2011) J Electron Mater 40:1533
20. Kliauga AM, Ferrante M (2000) J Mater Sci 35:4243. doi:10.1023/A:1004815830980
21. Asthana R, Singh M (2008) J Eur Ceram Soc 28:617
22. Kliauga AM, Travessa D, Ferrante M (2001) Mater Charact 46:65
23. Massalski TB, Okamoto H (1990) Binary alloy phase diagrams. Ohio, USA. Reprinted with permission of ASM International. All rights reserved. www.asminternational.org. Accessed 28 May 2013
24. Jin S, Duarte LI, Huang G, Leinenbach C (2012) Monatsh Chem 143:1263